



Published in final edited form as:

Exp Biol Med (Maywood). 2013 November 1; 238(11): 1265–1274. doi:10.1177/1535370213492693.

Geranylgeraniol suppresses the viability of human DU145 prostate carcinoma cells and the level of HMG CoA reductase

Nicolle V. Fernandes^{1,4}, Hoda Yeganehjoo¹, Rajasekhar Katuru¹, Russell A. DeBose-Boyd², Lindsey L. Morris², Renee Michon¹, Zhi-Ling Yu³, and Huanbiao Mo¹

¹Department of Nutrition and Food Sciences, Texas Woman's University, Denton, TX 76204, USA

²Howard Hughes Medical Institute and Department of Molecular Genetics, University of Texas Southwestern Medical Center, Dallas, TX 75390-9050, USA

³Center for Cancer and Inflammation Research, School of Chinese Medicine, Hong Kong Baptist University, Kowloon Tong, Hong Kong, China

⁴Department of Family and Consumer Sciences, Ball State University, Muncie, IN 47306, USA

Abstract

The rate-limiting enzyme of the mevalonate pathway, 3-hydroxy-3-methylglutaryl coenzyme A (HMG CoA) reductase, provides essential intermediates for the prenylation of nuclear lamins and Ras and dolichol-mediated glycosylation of growth factor receptors. The diterpene geranylgeraniol downregulates the level of HMG CoA reductase and suppresses the growth of human liver, lung, ovary, pancreas, colon, stomach, and blood tumors. We evaluated the growth-suppressive activity of geranylgeraniol in human prostate carcinoma cells. Geranylgeraniol induced dose-dependent suppression of the viability of human DU145 prostate carcinoma cells ($IC_{50} = 80 \pm 18 \mu\text{mol/L}$, $n = 5$) following 72-h incubations in 96-well plates. Cell cycle was arrested at the G1 phase with a concomitant decrease in cyclin D1 protein. Geranylgeraniol-induced apoptosis was detected by flow cytometric analysis, fluorescence microscopy following acridine orange and ethidium bromide dual staining, and caspase-3 activation. Geranylgeraniol-induced viability suppression was accompanied by concentration-dependent decrease in the level of HMG CoA reductase protein. As a nonsterol molecule that downregulates HMG CoA reductase in the presence of sterols, geranylgeraniol may have potential in the chemoprevention and/or therapy of human prostate cancer.

Keywords

Geranylgeraniol; prostate carcinoma; HMG CoA reductase; mevalonate; cell cycle; apoptosis

Copyright © 2013 by the Society for Experimental Biology and Medicine

Corresponding author: Huanbiao Mo. hmo@mail.twu.edu.

Author contributions: All authors participated in the design, interpretation of the studies and analysis of the data and review of the manuscript; NVF, HY, RK, LM, RM, and HM conducted the experiments, RAD supplied antibody to HMG CoA reductase and LPDS; HY, RAD, ZLY and HM wrote the manuscript.

Introduction

The estimated 23,000 isoprenoids are mevalonate-derived products of plant secondary metabolism.¹ Within this class of chemicals are the 'pure' isoprenoids with their entire structure derived from the 5-carbon isoprene unit. The tumor-suppressive activity of dietary pure isoprenoids encompassing the monoterpenes, sesquiterpenes, and diterpenes has been previously reviewed.²

The tumor-suppressive activity of dietary isoprenoids has been ascribed at least in part to the suppression of 3-hydroxy-3-methylglutaryl coenzyme A (HMG CoA) reductase activity, the rate-limiting activity in the mevalonate pathway. Mevalonate-derived intermediates, most notably farnesyl pyrophosphate (FPP) and geranylgeranyl pyrophosphate (GGPP), are essential for the posttranslational prenylation of Ras and nuclear lamins and dolichol-mediated glycosylation of insulin-like growth factor I (IGF-I) receptor³ that support growth. Among the pure isoprenoids is the sesquiterpene farnesol⁴ shown to downregulate HMG CoA reductase. A more recent study demonstrated that geranylgeraniol is more active than farnesol in inducing reductase degradation in human SV-589 immortalized fibroblasts expressing the SV40 large T antigen⁵; geranylgeraniol promotes the degradation of reductase following sterol-stimulated ubiquitination. Consequently, geranylgeraniol has been shown to suppress the growth of murine B16 melanoma cells,⁶ likely due to the reduced availability of FPP and GGPP. Our recent study showed that supplemental mevalonate, the product of HMG CoA reductase, attenuated geranylgeraniol-mediated growth suppression in murine B16 melanoma cells, further supporting geranylgeraniol-mediated reductase suppression. Nevertheless, the impact of geranylgeraniol on the level of HMG CoA reductase protein has not been shown in a tumor cell line.

In this study we evaluated the effect of geranylgeraniol on cell viability and HMG CoA reductase in human prostate carcinoma cells. Geranylgeraniol induced cell cycle arrest at the G1 phase and initiated apoptosis, effects accompanied by downregulation of HMG CoA reductase level. We chose the prostate cancer cells based on the following considerations. The use of statins, competitive inhibitors of HMG CoA reductase, has been associated with lower risk of prostate cancer.^{7,8} More recently, suppression of HMG CoA reductase and the processing of its transcriptional factor, sterol regulatory element binding protein 2 (SREBP-2), was correlated with reduced viability of human prostate cancer cells,⁹ suggesting that HMG CoA reductase may afford a viable target for intervention in prostate cancer.

Materials and methods

Chemicals

Geranylgeraniol was purchased from Sigma-Aldrich (St. Louis, MO, USA). Lovastatin was a gift from Merck Research Laboratories (Rahway, NJ, USA).

Cell viability assay

Human DU145 prostate carcinoma cells (HTB-81, ATCC, Manassas, VA, USA) were grown in Eagle's minimal essential medium (MEM) modified by ATCC to contain 1.0

mmol sodium pyruvate/L, 0.1 mmol nonessential amino acids/L, and 1.5 g sodium bicarbonate/L, supplemented with 10% fetal bovine serum (FBS, Hyclone Laboratories Inc., Logan, UT, USA) and 80 mg gentamycin/L. Cultures of the cells, seeded in 0.1 mL medium with 1000 cells/well in a 96-well plate, were incubated for 24 h at 37°C in a humidified atmosphere of 5% CO₂. At 24 h the medium was decanted from each well and 0.1 mL fresh medium containing geranylgeraniol was added. All cultures contained 1 mL/L each of ethyl alcohol. Incubation continued for additional 72 h. The 72-h cell populations following a quick rinse with 0.1 mL Hank's balanced salt solution (HBSS) were determined by adding 20 µL of CellTiter 96[®] Aqueous One Solution to each well; plates were held in the dark at 37°C for 2 h and then read at 490 nm with a SPECTRAmax[®] 190 multi-plate reader with SOFTmax[®] PRO version 3.0 (Molecular Devices, Sunnyvale, CA, USA). Absorbances from wells containing cell-free medium were used as baselines and were deducted from absorbances of other cell-containing wells. The IC₅₀ value is the concentration of geranylgeraniol required to suppress the net increase in cell number by 50%.

Cell cycle distribution

DU145 cells were seeded in 25 cm² flasks (Becton Dickinson Labware, Franklin Lakes, NJ, USA) at 1.5×10^6 cells/flask with 5 mL medium/flask and incubated for 24 h. Medium was then decanted and cultures replenished with medium containing geranylgeraniol that had been dissolved in ethyl alcohol. Following additional 24 - and 48-h incubations, adherent DU145 cells were harvested by trypsinization and pelleted by low-speed centrifugation. Cell pellets were fixed in 1 mL 70% ethanol at -20°C overnight and washed in 1 mL phosphate-buffered saline (PBS). Cells (5×10^5) were re-suspended in 500 µL PBS containing 0.5 mg RNase A (Sigma-Aldrich) and incubated at 37°C for 30 min. Following gentle mixing a 100 µL aliquot of propidium iodide (Sigma-Aldrich, 1 g/L in PBS containing 0.1% Triton X-100) was added. The cells were incubated in the dark at room temperature for 15 min and then held at 4°C in the dark for flow cytometric analysis.¹⁰ Aliquots of 1×10^4 cells were analyzed for DNA content using a BD FACSCaliber[™] flow cytometer (BD Biosciences, San Jose, CA, USA). The distribution of cells in the G1, S, and G2/M phases of the cell cycle was determined using MultiCycle AV software (Phoenix Flow Systems, San Diego, CA, USA).

Annexin V assay for apoptosis

DU145 cells were seeded in 25 cm² flasks (Becton Dickinson Labware) at 1.5×10^6 cells/flask with 5 mL medium/flask and incubated for 24 h. Medium was then decanted and cultures replenished with medium containing geranylgeraniol and lovastatin (pre-dissolved in dimethyl sulfoxide). Following additional 24-h incubation, adherent DU145 cells were harvested by trypsinization, combined with floaters and pelleted by low-speed centrifugation. Resuspended cells in 150 µL medium containing 1×10^4 cells were mixed with 50 µL of the Guava Nexin[™] reagent containing Annexin V-PE and Nexin 7-amino-actinomycin D (7-AAD), loaded onto the 96-well plate, and incubated at room temperature in the dark for 20 min. Samples containing 5×10^3 cells were analyzed by using a Guava EasyCyte flow cytometer (Guava Technologies, Inc., Hayward, CA, USA) with the Guava ExpressPlus program.^{10,11} Annexin V is a phospholipid-binding protein that has high affinity for phosphatidylserine¹² translocated from the internal surface to the outer surface of

cell membrane at the early stage of apoptosis.¹³ 7-AAD selectively permeates late stage apoptotic and dead cells. Therefore, cells that are viable (Annexin V⁻ and 7-AAD⁻), early apoptotic (Annexin V⁺ and 7-AAD⁻), late apoptotic (Annexin V⁺ and 7-AAD⁺) and dead cells with nuclear debris (Annexin V⁻ and 7-AAD⁺) can be separated and percentages of these cell populations quantified.

Acridine orange and ethidium bromide dual staining assay for apoptosis

Human DU145 prostate carcinoma cells were inoculated in 96-well plates with 2×10^3 cells per well and incubated for 24-h. Medium was then decanted and cultures replenished with medium containing geranylgeraniol and lovastatin. Following additional 24-h incubation, the media was decanted and 100 μ L cold PBS was added. A dye mixture (4 μ L) containing 50 μ g/mL acridine orange (Becton, Dickinson and Company, Sparks, MD, USA) and 50 μ g/mL ethidium bromide (Sigma-Aldrich) was added to each well. Following a 2-min staining the cells were observed under an Axiovert 200 M microscope (Carl Zeiss MicroImaging Inc., Thornwood, NY, USA) equipped with a FluoArc lamp, an AxioCam MRm digital camera system (Carl Zeiss), and AxioVision Rel. 4.3 program (Carl Zeiss). Representative fields of each well with green and red fluorescence emitted by acridine orange and ethidium bromide staining were captured using fluorescein isothiocyanate (FITC) and tetramethylrhodamine isothiocyanate (TRITC) filters, respectively.¹¹

Western blot

Following incubation with geranylgeraniol and lovastatin for 24 and 48 h, human DU145 prostate carcinoma cells were washed with 10 mL ice cold PBS twice and then 150 μ L of lysis buffer (50 mmol/L Tris-HCl, pH 8.8, 5 mmol/L EDTA, 1% SDS) containing freshly mixed 1% protease inhibitor cocktail (Sigma-Aldrich) was added to the flask. Cells were sonicated (Fisher Scientific) for 45 s and placed in a dry bath incubator (Boekel Scientific, Feasterville, PA, USA) at 90°C for 20 min.

For analysis of HMG CoA reductase, DU145 cells cultured in 10-cm dishes at 3.5×10^6 per dish were incubated in MEM media containing 10% FBS and 0–100 μ mol/L geranylgeraniol. Two additional groups of cells were incubated with MEM media supplemented with 10% lipoprotein deficient serum (LPDS); these cells were treated with either 10 mmol/L mevalonate in the presence of 1 μ g/mL of 25-hydroxycholesterol or 0.05 mmol/L mevalonate only. Following 24-h incubation the cells were scraped and membrane fractions obtained as previously reported.¹⁴

Protein concentration of each sample was determined with BCATM Protein Assay Kit (Pierce, Rockford, IL, USA). Samples containing 60 μ g proteins from whole cell lysates were mixed with Laemmli buffer (Bio-Rad Laboratories, Hercules, CA, USA) at 1:1 ratio (v/v) and boiled for 5 min before being loaded onto a Mini PROTEAN[®] 3 (Bio-Rad) electrophoresis unit with a 15% SDS-polyacrylamide gel. Membrane extracts (20 μ g proteins) were mixed with equal volume of buffer (62.5 mmol/L Tris-HCl, pH 6.8, 15% (w/v) SDS, 8 mol/L urea, 10% (v/v) glycerol, and 100 mmol/L dithiothreitol) and 1/6 volume of the 4 \times SDS loading buffer (150 mmol/L Tris-HCl, pH 6.8, 12% (w/v) SDS, 30% glycerol, 6% β -mercaptoethanol, and bromophenol blue) and incubated at 37°C for 20 min prior to loading to

an 8% SDS polyacrylamide gel. Western blot with monoclonal antibodies to cyclin D1, procaspase-3 (Cell Signaling Technology, Beverly, MA, USA) and HMG CoA reductase was performed as described previously.⁶

Statistics

One-way analysis of variance (ANOVA) and Kruskal-Wallis tests were performed to assess the differences between groups using Prism[®] 4.0 software (GraphPad Software Inc., San Diego, CA). Differences in means were analyzed by Dunnett's multiple comparison test unless specified otherwise. Two-way ANOVA was analyzed by SPSS version 19. Levels of significance were designated as $P < 0.05$.

Results

Figure 1 shows the concentration-dependent suppression of the viability of human DU145 prostate carcinoma cells by geranylgeraniol. Our previous study with murine B16 melanoma cells showed that geranylgeraniol induces cell cycle arrest at the G1 phase.⁶ We then evaluated the impact of geranylgeraniol on the cell cycle distribution of the DU145 cells (Figure 2). Following a 24-h incubation with geranylgeraniol the percentage of cells at the G1 phase increased from $50.0 \pm 2.0\%$ (control) to $56.7 \pm 2.5\%$ (50 $\mu\text{mol/L}$ geranylgeraniol), and $77.0 \pm 1.9\%$ (100 $\mu\text{mol/L}$ geranylgeraniol, $P < 0.01$), respectively. Conversely, the percentage of cells at the S phase decreased from $44.8 \pm 3.4\%$ (control) and $44.3 \pm 6.2\%$ (50 $\mu\text{mol/L}$ geranylgeraniol), respectively, to $19.5 \pm 1.0\%$ (100 $\mu\text{mol/L}$ geranylgeraniol, $P < 0.05$). Geranylgeraniol also induced G1 arrest in cells following 48-h incubation.

The G1 arrest induced by geranylgeraniol was accompanied by suppression of the expression of cyclin D1, a key regulator in the G1/S cell cycle progression.¹⁵ Following 48-h incubations with 100 $\mu\text{mol/L}$ geranylgeraniol, the level of cyclin D1 protein decreased significantly (Figure 3).

Previous studies have also shown that geranylgeraniol induces apoptosis in tumor cells, an effect we then evaluated in the DU145 cells using the Guava Nexin[™] assay with flow cytometry. Following a 24-h incubation with 0, 50, and 100 $\mu\text{mol/L}$ geranylgeraniol and 10 $\mu\text{mol/L}$ lovastatin, the percentage of viable cells (Figure 4) were 98.2 ± 0.4 , 97.9 ± 0.2 , 92.6 ± 0.4 ($P < 0.01$), and 96.1 ± 0.7 ($P < 0.01$), respectively. Concomitantly, treatment with geranylgeraniol and lovastatin increased the percentage of apoptotic cells. The percentage of early apoptotic cells in cells treated with 100 $\mu\text{mol/L}$ (0.9 ± 0.3 , $P < 0.05$) of geranylgeraniol was significantly higher than that in untreated cells (0.3 ± 0.2). Cells treated with 100 $\mu\text{mol/L}$ geranylgeraniol ($6.0 \pm 0.6\%$, $P < 0.01$) and 10 $\mu\text{mol/L}$ lovastatin ($2.8 \pm 0.8\%$, $P < 0.01$) had significantly higher late apoptosis rate than that of the control cells ($1.2 \pm 0.4\%$).

Geranylgeraniol- and lovastatin-induced apoptosis was confirmed by fluorescence microscopy (Figure 5) and procaspase-3 activation (Figure 6). In photomicrographs of DU145 cells (Figure 5) obtained by acridine orange and ethidium bromide dual staining, viable cells have acridine orange staining with normal cell morphology. Acridine orange and ethidium bromide stained cells with condensed nucleus are in early and late apoptosis stages, respectively.^{11,16} The ethidium bromide stained DU145 cells following a 24-h

incubation with 50 (Figure 5(g)) and 100 (Figure 5(h)) $\mu\text{mol/L}$ of geranylgeraniol and 10 (Figure 5(i)) and 20 (Figure 5(j)) $\mu\text{mol/L}$ of lovastatin were more visible than the control (Figure 5(f)). Arrows mark the red fluorescence emission from ethidium bromide staining shown in late apoptotic and necrotic cells induced by geranylgeraniol and lovastatin. Following 48-h incubations with 50 and 100 $\mu\text{mol/L}$ geranylgeraniol, the intensity of procaspase-3 decreased in a concentration-dependent manner (Figure 6); 100 $\mu\text{mol/L}$ geranylgeraniol induced procaspase-3 activation at 24-h. There was a concurrent appearance of the lower-molecular weight bands in geranylgeraniol-treated cells, indicating the cleavage of procaspase-3.

Our previous study suggested that geranylgeraniol-mediated growth suppression in melanoma cells may stem from the down-regulation of HMG CoA reductase. We then evaluate the impact of geranylgeraniol on the level of HMG CoA reductase in DU145 cells (Figure 7). Following 24-h incubation in medium supplemented with 10% LPDS, there was a high level of reductase expression due to the lack of sterol feedback inhibition. Mevalonate (10 mmol/L) and 25-hydroxycholesterol (1 $\mu\text{g/mL}$) reduced reductase to an undetectable level, consistent with the notion that sterols and non-sterols accelerate the degradation of reductase.¹⁷ When DU145 cells were grown in medium supplemented with 10% FBS, the reductase level was lower than that in cells grown in medium supplemented with LPDS. Geranylgeraniol at 75 and 100 $\mu\text{mol/L}$ further reduced the level of reductase ($P < 0.05$).

Discussion

In this study, we have shown for the first time that geranylgeraniol suppresses the viability of human prostate DU145 carcinoma cells. The prostate cancer cells ($\text{IC}_{50} = 80 \mu\text{mol/L}$) appear to be more resistant than the murine B16 melanoma cells ($\text{IC}_{50} = 55 \mu\text{mol/L}$) we previously evaluated⁶ based on the IC_{50} values. Nevertheless, this IC_{50} value for prostate cancer cells still falls between those determined for human HuH-7 hepatoma cells ($\text{IC}_{50} = 10 \mu\text{mol/L}$)¹⁸ and human H460 lung adenocarcinoma cells ($\text{IC}_{50} = 400 \mu\text{mol/L}$)¹⁹ that are among a list of tumor cells⁶ sensitive to geranylgeraniol-mediated growth suppression.

The geranylgeraniol-mediated cell cycle arrest at the G1 phase and the downregulation of cyclin D1 are reminiscent of the impacts in B16 melanoma cells.⁶ These results are consistent with previous findings that mevalonate deprivation induced G1 arrest²⁰ in human prostate cancer cells, downregulated the expression of cyclin D1,²¹ and upregulated the expressions of p21^{22,23} and p27,²²⁻²⁴ two proteins involved in regulating G1/S transition. The monoterpenes perillyl alcohol and geraniol and sesquiterpene farnesol also induced G1 arrest and increase in p27 expression.²⁵

In addition to cell cycle arrest, geranylgeraniol-induced apoptosis also contributed to growth inhibition. Geranylgeraniol-induced caspase-3 activation is in agreement with previous observations in human U937²⁶ and HL60²⁷ leukemia cells and human HuH-7 hepatoma cells.¹⁸ Inhibition of protein kinase C (PKC),²⁸ activation of c-Jun N-terminal kinases (JNK),²⁹ and release of cytochrome c³⁰ have been implicated in geranylgeraniol-induced apoptosis.

These effects of geranylgeraniol on cell viability, cell cycle arrest and apoptosis were concurrent with the downregulation of HMG CoA reductase (Figure 7). HMG CoA reductase is under a multivalent regulation mediated by sterols and non-sterol isoprenoids.³ Mevalonate-derived nonsterol isoprenoids have been suggested to accelerate the sterol-stimulated degradation of HMG CoA reductase, an important part of the reductase regulation. In our hands 25-hydroxycholesterol and mevalonate reduced reductase to below minimal detectable level, suggesting that this regulatory mechanism mediated by sterols and nonsterol isoprenoids persists in human prostate cancer cells. Several in vitro and in vivo studies suggested that farnesol is the signal for mammalian HMG CoA reductase degradation.^{4,31,32} In contrast to studies using Chinese Hamster Ovary (CHO) cells⁴ treated with compactin and Met-18b-2 cells³² with mevastatin showing farnesol as the HMG CoA reductase regulator, others found that a 1000-fold increase in rat hepatic farnesol level did not affect the turnover rate of hepatic HMG CoA reductase.³³ In addition, the apparent farnesol-induced reductase degradation may be caused by detergent-insoluble reductase precipitated by farnesol that was not detectable by immunoprecipitation.⁴

More recent evidence suggested that geranylgeraniol might be the nonsterol to mediate HMG CoA reductase degradation. Geranylgeraniol (125 $\mu\text{mol/L}$) suppressed acetate incorporation into cholesterol by 70% in NIH3T3 cells, an effect greater than that induced by a higher concentration (167 $\mu\text{mol/L}$) of farnesol.³⁴ Geranylgeraniol was also more potent than farnesol in suppressing HMG CoA reductase in human mevalonate kinase-deficient fibroblasts³⁵ and human A549 lung carcinoma cells³⁶ and in inducing HMG CoA reductase degradation, an effect amplified by sterols, in human SV-589 immortalized fibroblasts.⁵ In the presence of sterols, reductase is ubiquitinated but not degraded; supplemental geranylgeraniol (10, 30 and 100 $\mu\text{mol/L}$) and to much less extent farnesol stimulated the extraction of reductase from endoplasmic reticulum and its degradation by the proteasome.⁵ It was postulated that geranylgeraniol is converted to GGPP, which is then used to prenylate a G protein such as Rab that is involved in vesicular transport.³⁷ In CHO cells farnesyl derivatives – farnesyl acetate and ethyl farnesyl ether – caused the degradation of HMG CoA reductase; Bradfute and Simoni³¹ postulated that these compounds directly induce the degradation because the mevalonate flux had been inhibited by statins. Later Song et al.³⁸ showed that lanosterol and 24, 25-dihydrolanosterol, metabolites that accumulated when the farnesyl derivatives inhibited its conversion to cholesterol, accelerated the degradation of HMG CoA reductase. Farnesyl derivatives may have indirectly induced the degradation of HMG CoA reductase through lanosterol and 24, 25-dihydrolanosterol accumulation.

In addition, our quantitative real-time PCR analysis showed no significant changes in the mRNA levels of HMG CoA reductase in DU145 cells following 24-h incubations with 0, 25, 50, 75, and 100 $\mu\text{mol/L}$ of geranylgeraniol (data not shown), suggesting a posttranscriptional downregulation of reductase.

Consistent with geranylgeraniol-mediated downregulation of HMG CoA reductase, geranylgeraniol ($\text{IC}_{50} = 25 \mu\text{mol/L}$) was more potent than farnesol ($\text{IC}_{50} = 39 \mu\text{mol/L}$) in suppressing the growth of human MIA PaCa-2 pancreatic adenocarcinoma cells.³⁹ Geranylgeraniol was also a more active apoptosis inducer than farnesol in HL-60 cells⁴⁰ and human A549 lung carcinoma cells.^{36,41} Moreover, geranylgeraniol also shares a striking

similarity with the competitive inhibitor of HMG CoA reductase, lovastatin, in inducing cell cycle arrest and apoptosis in DU145 cells (Figures 4 and 5). This similarity is in accordance with our previous observation that mevalonate attenuated geranylgeraniol-induced growth inhibition in B16 melanoma cells.⁶ The activation of PKC, an upregulator of HMG CoA reductase mRNA level,⁴² prevents geranylgeraniol-induced apoptosis,²⁸ lending further support to the role of HMG CoA reductase in mediating the geranylgeraniol action.

The geranylgeraniol-mediated HMG CoA reductase down-regulation and apoptosis observed herein present apparent contradictions to reports that geranylgeraniol prevented lovastatin-induced apoptosis in prostate tumor cells⁴³ and benign prostatic hyperplasia stromal cells.⁴⁴ In the latter studies, however, statin-mediated sterol deprivation may have obstructed the role of geranylgeraniol in accelerating sterol-dependent HMG CoA reductase degradation.⁵ As a consequence, the conversion from geranylgeraniol to GGPP³⁷ filled a void of prenyl protein transferase substrates and prevented apoptosis.

Based on the current results, we propose a working model for geranylgeraniol-mediated growth suppression (Figure 8). By downregulating the level of HMG CoA reductase, geranylgeraniol downsizes the pools of mevalonate and the downstream farnesyl- and geranylgeranyl-pyrophosphates; consequently, the prenylation of Ras and nuclear lamins and glycosylation of IGF-I receptor are ablated, impeding cell growth. In vivo studies using models of prostate cancer are warranted to validate the growth-suppressive activity of geranylgeraniol; lack of such studies precludes discussion on the physiological applicability of the concentrations used herein. Nevertheless, gavage feeding of geranylgeraniol to Wistar rats suppressed chemically initiated hepatocarcinogenesis and, more relevant to our study, reduced plasma cholesterol level⁴⁵; the latter is a potential outcome of HMG CoA reductase downregulation. It remains to be seen whether the synergistic impact of geranylgeraniol and other mevalonate suppressors such as the tocotrienols⁶ persists in prostate cancer cells and whether such impact is mediated by downregulation of HMG CoA reductase. Geranylgeraniol may be a new weapon in the arsenal of mevalonate-suppressive isoprenoids in the fight against prostate cancer.

Acknowledgments

This work was partially supported by Texas Department of Agriculture Food and Fiber Research Program, Texas Woman's University Research Enhancement Program, Summer Stipend Award and Human Nutrition Research Fund, American River Nutrition, Inc., National Institute of Health (GM090216), and the Howard Hughes Medical Institutes.

References

1. Bach TJ. Some new aspects of isoprenoid biosynthesis in plants—a review. *Lipids*. 1995; 30:191–202. [PubMed: 7791527]
2. Mo H, Elson CE. Studies of the isoprenoid-mediated inhibition of mevalonate synthesis applied to cancer chemotherapy and chemoprevention. *Exp Biol Med (Maywood)*. 2004; 229:567–85. [PubMed: 15229351]
3. Goldstein JL, Brown MS. Regulation of the mevalonate pathway. *Nature*. 1990; 343:425–30. [PubMed: 1967820]

4. Meigs TE, Roseman DS, Simoni RD. Regulation of 3-hydroxy-3-methylglutaryl-coenzyme A reductase degradation by the nonsterol mevalonate metabolite farnesol in vivo. *J Biol Chem.* 1996; 271:7916–22. [PubMed: 8626470]
5. Sever N, Song BL, Yabe D, Goldstein JL, Brown MS, DeBose-Boyd RA. Insig-dependent ubiquitination and degradation of mammalian 3-hydroxy-3-methylglutaryl-CoA reductase stimulated by sterols and geranylgeraniol. *J Biol Chem.* 2003; 278:52479–90. [PubMed: 14563840]
6. Katuru R, Fernandes NV, Elfakhani M, Dutta D, Mills N, Hynds DL, King C, Mo H. Mevalonate depletion mediates the suppressive impact of geranylgeraniol on murine B16 melanoma cells. *Exp Biol Med (Maywood).* 2011; 236:604–13. [PubMed: 21540247]
7. Graaf MR, Beiderbeck AB, Egberts AC, Richel DJ, Guchelaar HJ. The risk of cancer in users of statins. *J Clin Oncol.* 2004; 22:2388–94. [PubMed: 15197200]
8. Osmak M. Statins and cancer: current and future prospects. *Cancer Lett.* 2012; 324:1–12. [PubMed: 22542807]
9. Krycer JR, Phan L, Brown AJ. A key regulator of cholesterol homeostasis, SREBP-2, can be targeted in prostate cancer cells with natural products. *Biochem J.* 2012; 446:191–201. [PubMed: 22657538]
10. Fernandes N, Jung M, Daoud A, Mo H. Biphenylalkylacetylhydroquinone ethers suppress the proliferation of murine B16 melanoma cells. *Anticancer Res.* 2008; 28:1005–12. [PubMed: 18507048]
11. Hussein D, Mo H. d- δ -Tocotrienol-mediated suppression of the proliferation of human PANC-1, MIA PaCa2 and BxPC-3 pancreatic carcinoma cells. *Pancreas.* 2009; 38:e124–36. [PubMed: 19346993]
12. Andree HA, Reutelingsperger CP, Hauptmann R, Hemker HC, Hermens WT, Willems GM. Binding of vascular anticoagulant alpha (VAC alpha) to planar phospholipid bilayers. *J Biol Chem.* 1990; 265:4923–8. [PubMed: 2138622]
13. Fadok VA, Voelker DR, Campbell PA, Cohen JJ, Bratton DL, Henson PM. Exposure of phosphatidylserine on the surface of apoptotic lymphocytes triggers specific recognition and removal by macrophages. *J Immunol.* 1992; 148:2207–16. [PubMed: 1545126]
14. Sever N, Yang T, Brown MS, Goldstein JL, DeBose-Boyd RA. Accelerated degradation of HMG CoA reductase mediated by binding of insig-1 to its sterol-sensing domain. *Mol Cell.* 2003; 11:25–33. [PubMed: 12535518]
15. Massague J. G1 cell-cycle control and cancer. *Nature.* 2004; 432:298–306. [PubMed: 15549091]
16. Fernandes NV, Guntipalli PK, Mo H. d- δ -Tocotrienol-mediated cell cycle arrest and apoptosis in human melanoma cells. *Anticancer Res.* 2010; 30:4937–44. [PubMed: 21187473]
17. DeBose-Boyd RA. Feedback regulation of cholesterol synthesis: sterol-accelerated ubiquitination and degradation of HMG CoA reductase. *Cell Res.* 2008; 18:609–21. [PubMed: 18504457]
18. Takeda Y, Nakao K, Nakata K, Kawakami A, Ida H, Ichikawa T, Shigeno M, Kajiya Y, Hamasaki K, Kato Y, Eguchi K. Geranylgeraniol, an intermediate product in mevalonate pathway, induces apoptotic cell death in human hepatoma cells: death receptor-independent activation of caspase-8 with down-regulation of Bcl-xL expression. *Jpn J Cancer Res.* 2001; 92:918–25. [PubMed: 11572758]
19. Joo JH, Liao G, Collins JB, Grissom SF, Jetten AM. Farnesol-induced apoptosis in human lung carcinoma cells is coupled to the endoplasmic reticulum stress response. *Cancer Res.* 2007; 67:7929–36. [PubMed: 17699800]
20. Lee SJ, Ha MJ, Lee J, Nguyen P, Choi YH, Pirnia F, Kang WK, Wang XF, Kim SJ, Trepel JB. Inhibition of the 3-hydroxy-3-methylglutaryl-coenzyme A reductase pathway induces p53-independent transcriptional regulation of p21(WAF1/CIP1) in human prostate carcinoma cells. *J Biol Chem.* 1998; 273:10618–23. [PubMed: 9553123]
21. Park C, Lee I, Kang WK. Lovastatin-induced E2F-1 modulation and its effect on prostate cancer cell death. *Carcinogenesis.* 2001; 22:1727–31. [PubMed: 11577016]
22. Shibata MA, Kavanaugh C, Shibata E, Abe H, Nguyen P, Otsuki Y, Trepel JB, Green JE. Comparative effects of lovastatin on mammary and prostate oncogenesis in transgenic mouse models. *Carcinogenesis.* 2003; 24:453–9. [PubMed: 12663504]

23. Rao S, Porter DC, Chen X, Herliczek T, Lowe M, Keyomarsi K. Lovastatin-mediated G1 arrest is through inhibition of the proteasome, independent of hydroxymethyl glutaryl-CoA reductase. *Proc Natl Acad Sci U S A*. 1999; 96:7797–802. [PubMed: 10393901]
24. Laufs U, Marra D, Node K, Liao JK. 3-Hydroxy-3-methylglutaryl-CoA reductase inhibitors attenuate vascular smooth muscle proliferation by preventing rho GTPase-induced down-regulation of p27(Kip1). *J Biol Chem*. 1999; 274:21926–31. [PubMed: 10419514]
25. Wiseman DA, Werner SR, Crowell PL. Cell cycle arrest by the isoprenoids perillyl alcohol, geraniol, and farnesol is mediated by p21(Cip1) and p27(Kip1) in human pancreatic adenocarcinoma cells. *J Pharmacol Exp Ther*. 2007; 320:1163–70. [PubMed: 17138864]
26. Masuda Y, Nakaya M, Nakajo S, Nakaya K. Geranylgeraniol potently induces caspase-3-like activity during apoptosis in human leukemia U937 cells. *Biochem Biophys Res Commun*. 1997; 234:641–5. [PubMed: 9175767]
27. Polverino AJ, Patterson SD. Selective activation of caspases during apoptotic induction in HL-60 cells. Effects of a tetrapeptide inhibitor. *J Biol Chem*. 1997; 272:7013–21. [PubMed: 9054391]
28. Masuda Y, Yoda M, Ohizumi H, Aiuchi T, Watabe M, Nakajo S, Nakaya K. Activation of protein kinase C prevents induction of apoptosis by geranylgeraniol in human leukemia HL60 cells. *Int J Cancer*. 1997; 71:691–7. [PubMed: 9178828]
29. Masuda Y, Nakaya M, Aiuchi T, Hashimoto S, Nakajo S, Nakaya K. The mechanism of geranylgeraniol-induced apoptosis involves activation, by a caspase-3-like protease, of a c-jun N-terminal kinase signaling cascade and differs from mechanisms of apoptosis induced by conventional chemotherapeutic drugs. *Leuk Res*. 2000; 24:937–50. [PubMed: 11086177]
30. Shibayama-Imazu T, Sakairi S, Watanabe A, Aiuchi T, Nakajo S, Nakaya K. Vitamin K(2) selectively induced apoptosis in ovarian TYK-nu and pancreatic MIA PaCa-2 cells out of eight solid tumor cell lines through a mechanism different from geranylgeraniol. *J Cancer Res Clin Oncol*. 2003; 129:1–11. [PubMed: 12618894]
31. Bradfute DL, Simoni RD. Non-sterol compounds that regulate cholesterol synthesis. Analogues of farnesyl pyrophosphate reduce 3-hydroxy-3-methylglutaryl-coenzyme A reductase levels. *J Biol Chem*. 1994; 269:6645–50. [PubMed: 8120018]
32. Correll CC, Ng L, Edwards PA. Identification of farnesol as the non-sterol derivative of mevalonic acid required for the accelerated degradation of 3-hydroxy-3-methylglutaryl-coenzyme A reductase. *J Biol Chem*. 1994; 269:17390–3. [PubMed: 8021239]
33. Keller RK, Zhao Z, Chambers C, Ness GC. Farnesol is not the nonsterol regulator mediating degradation of HMG-CoA reductase in rat liver. *Arch Biochem Biophys*. 1996; 328:324–30. [PubMed: 8645011]
34. Ownby SE, Hohl RJ. Farnesol and geranylgeraniol: prevention and reversion of lovastatin-induced effects in NIH3T3 cells. *Lipids*. 2002; 37:185–92. [PubMed: 11908910]
35. Houten SM, Schneiders MS, Wanders RJ, Waterham HR. Regulation of isoprenoid/cholesterol biosynthesis in cells from mevalonate kinase-deficient patients. *J Biol Chem*. 2003; 278:5736–43. [PubMed: 12477733]
36. Miquel K, Pradines A, Favre G. Farnesol and geranylgeraniol induce actin cytoskeleton disorganization and apoptosis in A549 lung adenocarcinoma cells. *Biochem Biophys Res Commun*. 1996; 225:869–76. [PubMed: 8780704]
37. Seabra MC, Mules EH, Hume AN. Rab GTPases, intracellular traffic and disease. *Trends Mol Med*. 2002; 8:23–30. [PubMed: 11796263]
38. Song BL, Javitt NB, DeBose-Boyd RA. Insig-mediated degradation of HMG CoA reductase stimulated by lanosterol, an intermediate in the synthesis of cholesterol. *Cell Metab*. 2005; 1:179–89. [PubMed: 16054061]
39. Burke YD, Stark MJ, Roach SL, Sen SE, Crowell PL. Inhibition of pancreatic cancer growth by the dietary isoprenoids farnesol and geraniol. *Lipids*. 1997; 32:151–6. [PubMed: 9075204]
40. Ohizumi H, Masuda Y, Nakajo S, Sakai I, Ohsawa S, Nakaya K. Geranylgeraniol is a potent inducer of apoptosis in tumor cells. *J Biochem (Tokyo)*. 1995; 117:11–3. [PubMed: 7775375]
41. Miquel K, Pradines A, Terce F, Selmi S, Favre G. Competitive inhibition of choline phosphotransferase by geranylgeraniol and farnesol inhibits phosphatidylcholine synthesis and

- induces apoptosis in human lung adenocarcinoma A549 cells. *J Biol Chem.* 1998; 273:26179–86. [PubMed: 9748300]
42. Chakrabarti R, Engleman EG. Interrelationships between mevalonate metabolism and the mitogenic signaling pathway in T lymphocyte proliferation. *J Biol Chem.* 1991; 266:12216–22. [PubMed: 1712015]
43. Ghosh PM, Ghosh-Choudhury N, Moyer ML, Mott GE, Thomas CA, Foster BA, Greenberg NM, Kreisberg JI. Role of RhoA activation in the growth and morphology of a murine prostate tumor cell line. *Oncogene.* 1999; 18:4120–30. [PubMed: 10435593]
44. Padayatty SJ, Marcelli M, Shao TC, Cunningham GR. Lovastatin-induced apoptosis in prostate stromal cells. *J Clin Endocrinol Metab.* 1997; 82:1434–9. [PubMed: 9141529]
45. de Moura Espindola R, Mazzantini RP, Ong TP, de Conti A, Heidor R, Moreno FS. Geranylgeraniol and β -ionone inhibit hepatic preneoplastic lesions, cell proliferation, total plasma cholesterol and DNA damage during the initial phases of hepatocarcinogenesis, but only the former inhibits NF- κ B activation. *Carcinogenesis.* 2005; 26:1091–9. [PubMed: 15718255]

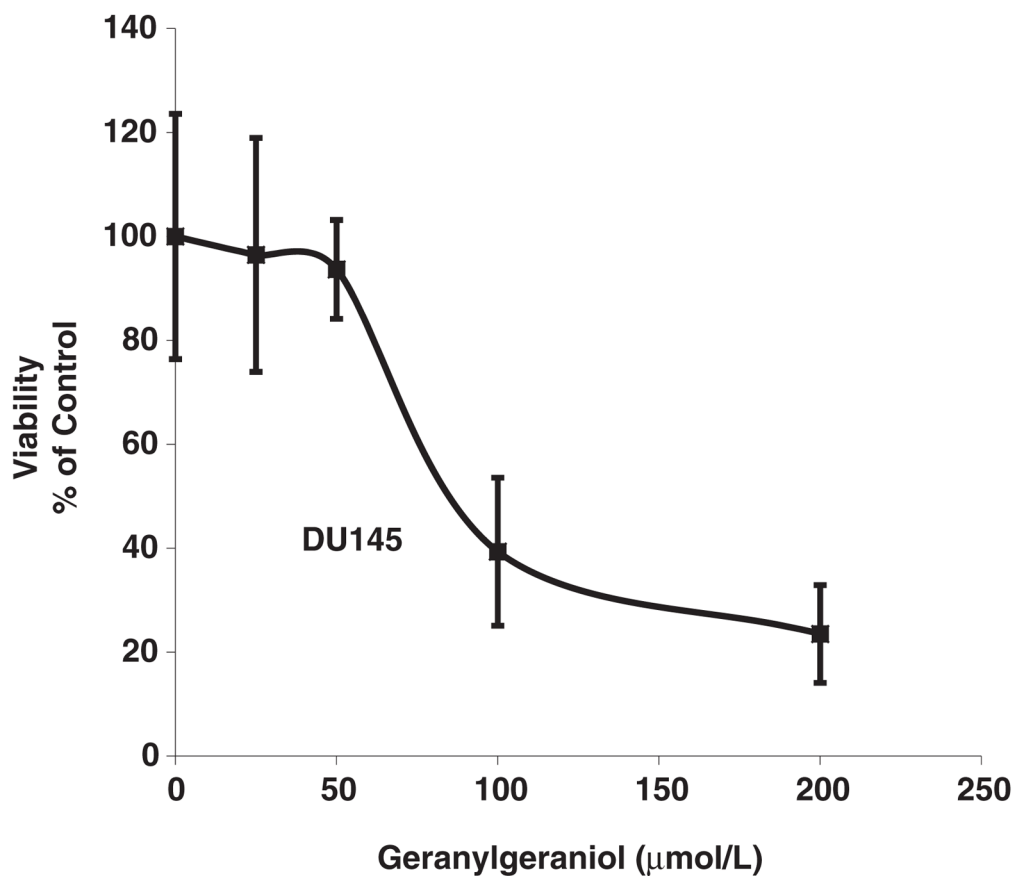


Figure 1.

A representative growth curve showing the concentration-dependent impact of geranylgeraniol on the viability of human DU145 prostate carcinoma cells. Cells were cultured and incubated with geranylgeraniol for 72 h before cell viability was measured by CellTiter 96[®] Aqueous One Solution. Values are mean \pm SD, $n = 4$

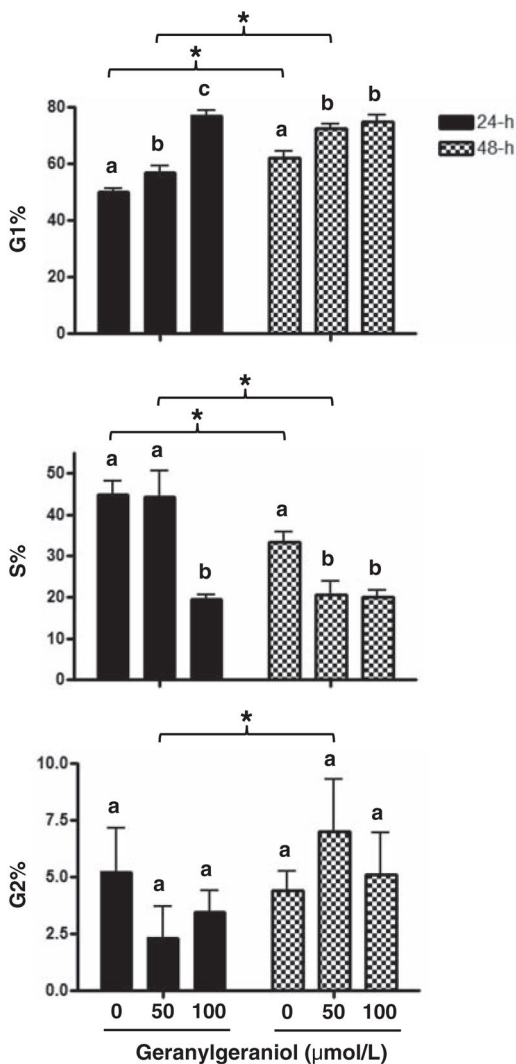


Figure 2.

The impact of geranylgeraniol on the cell cycle distribution of human DU145 prostate carcinoma cells shown by the percentages of cells in G1, S, and G2 phases of the cell cycle following 24- and 48-h incubations with 0, 50 and 100 μmol/L geranylgeraniol.

Values are mean ± SD, *n* = 3. Values not sharing a common letter within a time point or indicated by an asterisk are different based on two-way ANOVA (*P* < 0.05)

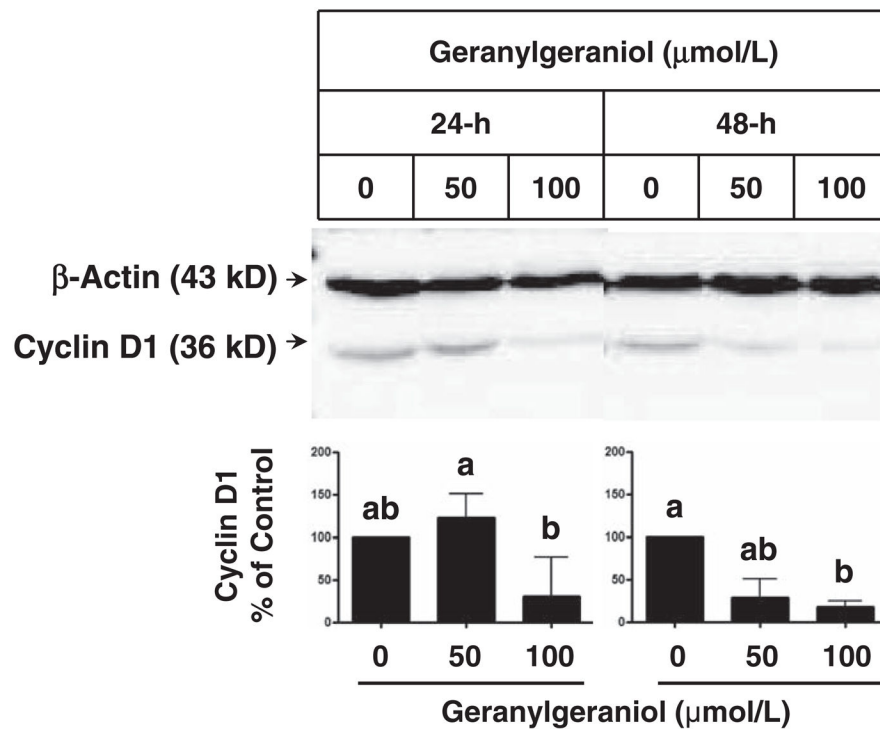


Figure 3.

The impact of geranylgeraniol on the expression of cyclin D1 in human DU145 prostate carcinoma cells following 24- and 48-h incubations. Cell lysates were subjected to Western blot procedures and blots were detected by chemiluminescence. Representative blots from three experiments are shown. Values in the bar graphs for the level of cyclin D1 protein normalized to that of β -actin are mean and range, $n = 4$. Differences between treated groups were analyzed by Kruskal–Wallis test with Dunn’s Multiple Comparison test. Values not sharing a common letter are different ($P < 0.05$)

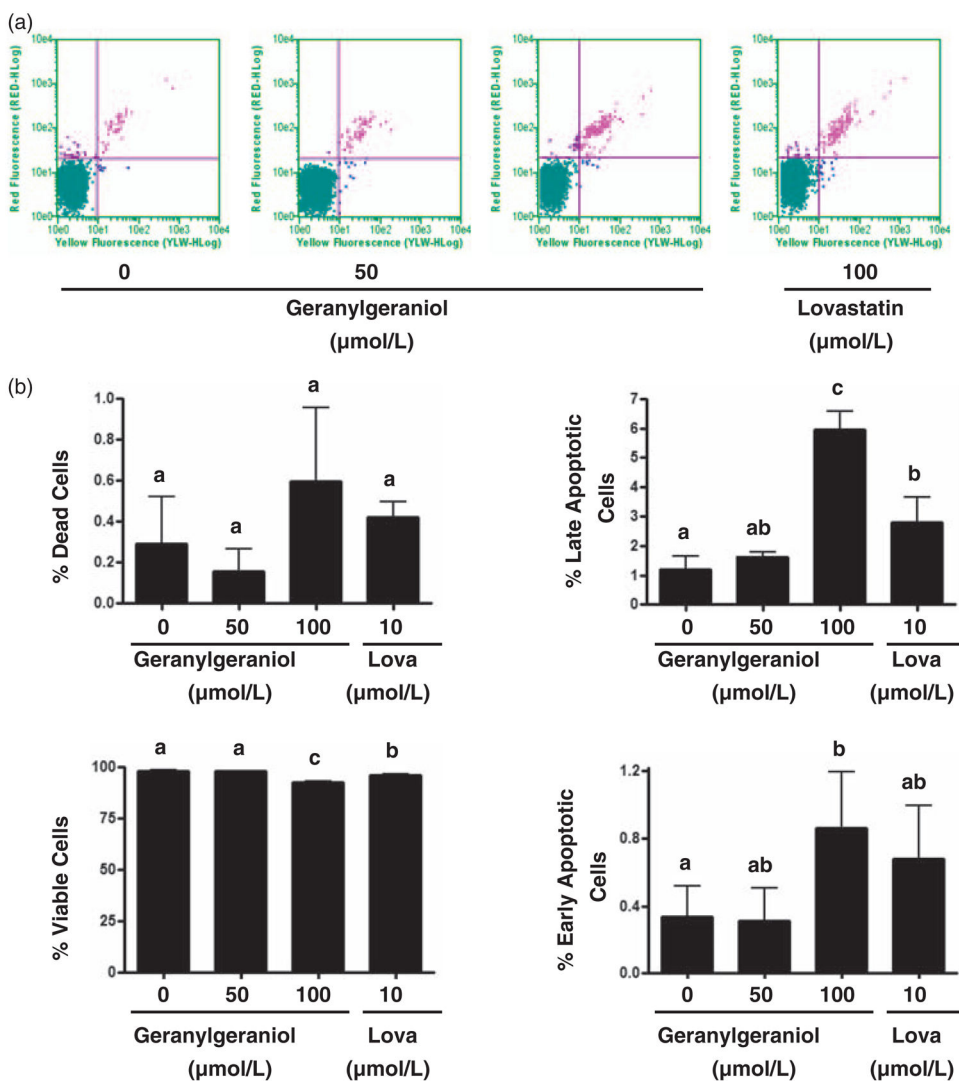


Figure 4.

The impact of geranylgeraniol and lovastatin (Lova) on the initiation of apoptosis in human DU145 prostate carcinoma cells. (a) DU145 cells were incubated with geranylgeraniol (0, 50, and 100 μmol/L) and lovastatin (10 μmol/L) for 24 h and then analyzed by flow cytometry using the Guava Nexin™ Assay. Cells in the lower left (Annexin V-/-AAD-), the lower right (Annexin V +/7-AAD-), the upper right (Annexin V+/7-AAD+) and the upper left (Annexin V-/-7-AAD+) quadrants represent viable, early apoptotic, late apoptotic, and dead cells, respectively. (b) The percentages of cells in each of the four quadrants as shown in part (a). Values are mean ± SD, *n* = 3. Differences between treated groups were analyzed by one-way ANOVA with Tukey's Multiple Comparison test. Values not sharing a common letter are different (*P* < 0.05). (A color version of this figure is available in the online journal).

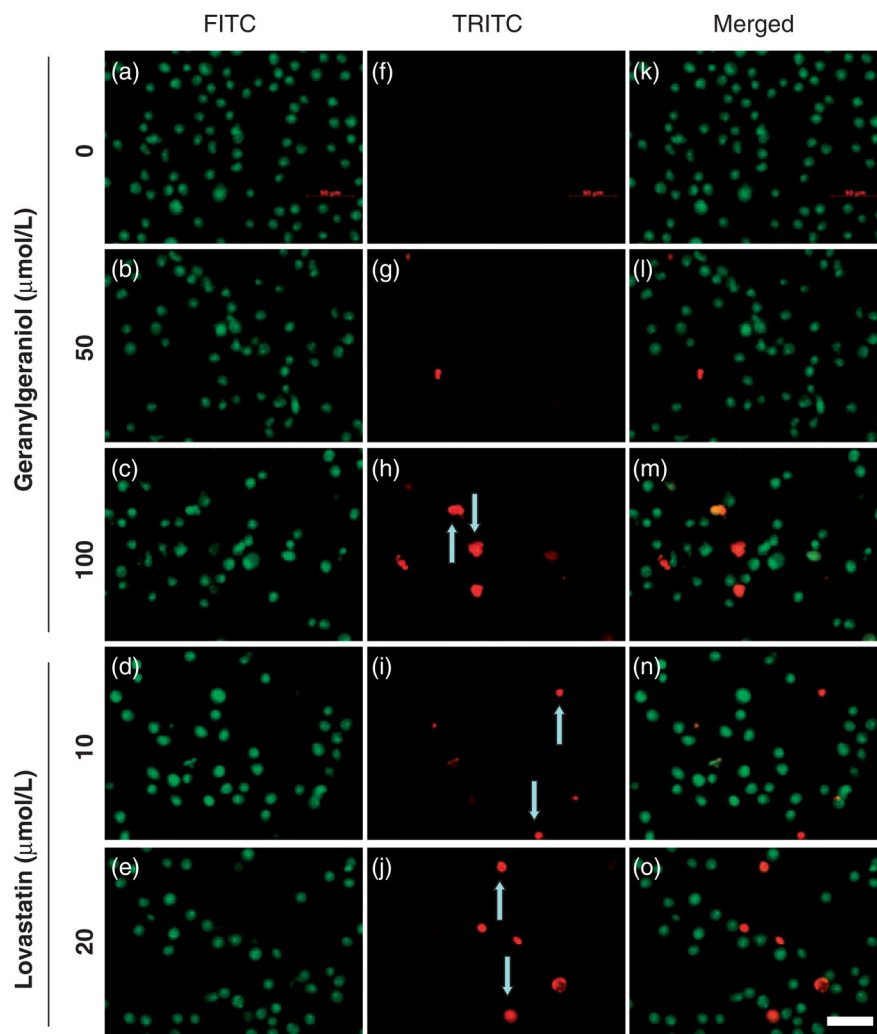


Figure 5.

Photomicrographs of human DU145 prostate carcinoma cells showing the geranylgeraniol- and lovastatin-initiated apoptosis detected by acridine orange and ethidium bromide dual staining. DU145 cells were incubated with 0 (a, f and k), 50 (b, g and l) and 100 (c, h and m) $\mu\text{mol/L}$ geranylgeraniol and 10 (d, i and n) and 20 (e, j and o) $\mu\text{mol/L}$ lovastatin for 24 h. Photomicrographs of the same fields were taken under fluorescence microscope with a FITC (a–e) or TRITC (f–j) filter and then merged (k–o). Arrows mark the red fluorescence emission from ethidium bromide staining shown in late apoptotic and necrotic cells induced by geranylgeraniol and lovastatin. The scale bar (o) represents 50 μm . (A color version of this figure is available in the online journal).

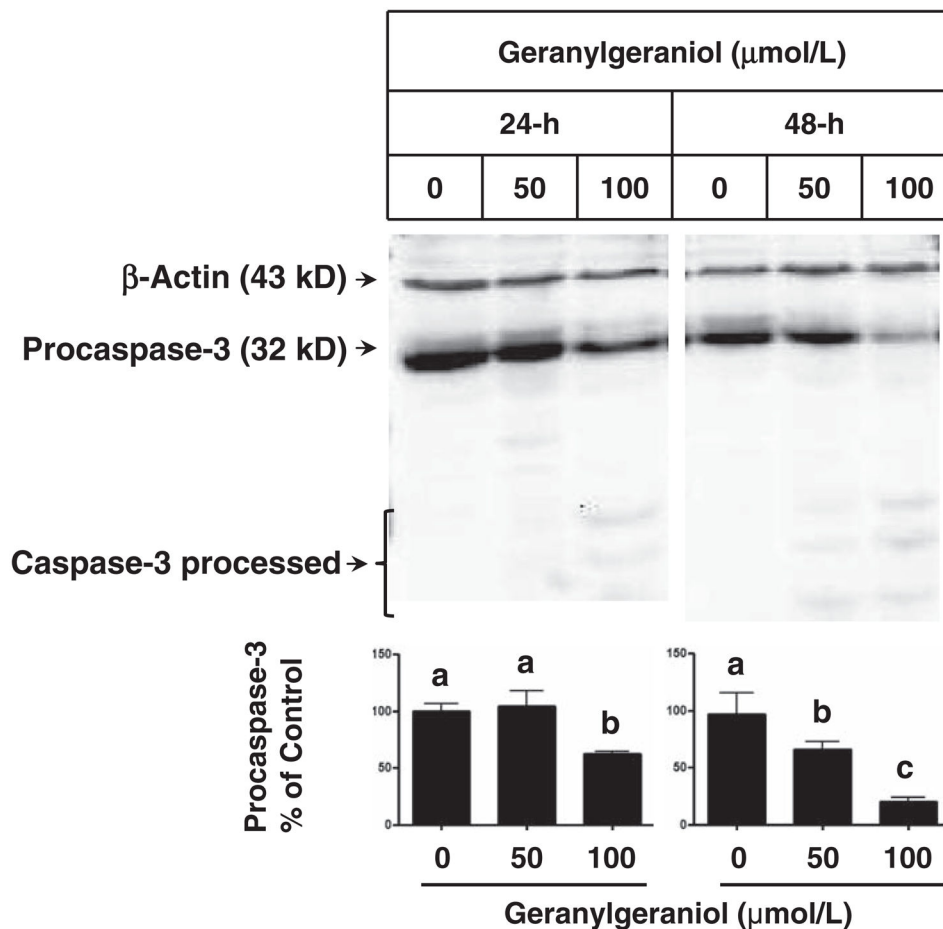


Figure 6.

The impact of geranylgeraniol on the activation of procaspase-3 in human DU145 prostate carcinoma cells following 24- and 48-h incubations. Cell lysates were subjected to Western blot procedures and blots were detected by chemiluminescence. Representative blots from more than three experiments are shown. Values in the bar graphs for the level of procaspase-3 protein normalized to that of β -actin are mean \pm SD, $n = 3$. Differences between treated groups were analyzed by one-way ANOVA with Tukey's Multiple Comparison test. Values not sharing a common letter are different ($P < 0.05$)

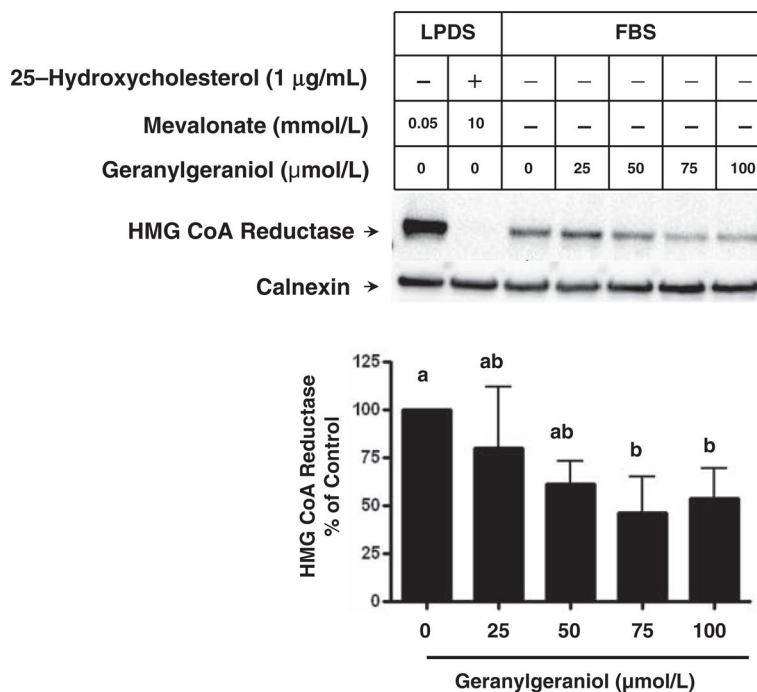


Figure 7.

The impact of geranylgeraniol on the level of HMG CoA reductase protein in human DU145 prostate carcinoma cells. DU145 cells were incubated with medium containing 10% LPDS supplemented with mevalonate (0.05 or 10 mmol/L) in the absence (–) or presence (+) of 25-hydroxycholesterol (1 $\mu\text{g/mL}$) as indicated, or medium containing 10% FBS and 0–100 $\mu\text{mol/L}$ geranylgeraniol for 24 h. Cells were lysed and membrane fractions were subjected to SDS-PAGE and Western blot with antibodies against HMG CoA reductase and calnexin, a marker for endoplasmic reticulum protein. Values in the bar graph for the level of HMG CoA reductase protein normalized to that of calnexin are mean \pm SD, $n = 4$. Differences between treated groups were analyzed by one-way ANOVA with Tukey's Multiple Comparison test. Values not sharing a common letter are different ($P < 0.05$)

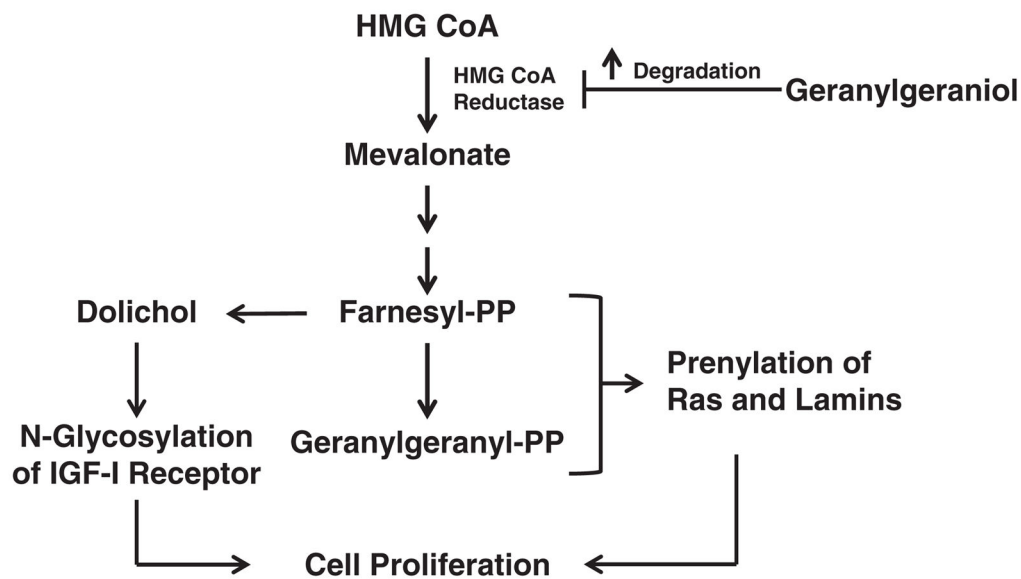


Figure 8.

Proposed mechanism of action for geranylgeraniol. The mevalonate pathway provides FPP and GGPP for the post-translational modification of Ras, lamins and IGF-I receptor, proteins required for cell viability. Geranylgeraniol downregulates the level of HMG CoA reductase, the rate-limiting enzyme in the mevalonate pathway and limits the pool size of FPP and GGPP. Consequently, geranylgeraniol reduces cell viability by inducing cell cycle arrest and apoptosis